

## Structure and production of lambda baryons

C. Boros

*Department of Physics and Mathematical Physics and Special Research Center for the Subatomic Structure of Matter,  
University of Adelaide, Adelaide 5005, Australia*

J. T. Londergan

*Department of Physics and Nuclear Theory Center, Indiana University, Bloomington, Indiana 47408*

A. W. Thomas

*Department of Physics and Mathematical Physics and Special Research Center for the Subatomic Structure of Matter,  
University of Adelaide 5005, Australia*

(Received 5 August 1999; published 7 December 1999)

We discuss the quark parton structure of the  $\Lambda$  baryon and the fragmentation of quarks into  $\Lambda$  baryons. We show that the hyperfine interaction, responsible for the  $\Delta$ - $N$  and  $\Sigma^0$ - $\Lambda$  mass splittings, leads not only to sizable  $SU(3)$  and  $SU(6)$  symmetry breaking in the quark distributions of the  $\Lambda$ , but also to significant polarized non-strange quark distributions. The same arguments suggest flavor asymmetric quark fragmentation functions and non-zero polarized non-strange quark fragmentation functions. The calculated fragmentation functions give a good description of all measured observables. We predict significant positive  $\Lambda$  polarization in semi-inclusive DIS experiments while models based on  $SU(3)$  flavor symmetry predict zero or negative  $\Lambda$  polarization. Our approach also provides a natural explanation for the dependence of the maximum of the  $\xi = \ln(1/z)$  spectrum on the mass of the particles produced in  $e^+e^-$  annihilation.

PACS number(s): 13.87.Fh, 13.85.Ni, 13.88.+e

### I. INTRODUCTION

An impressive amount of information on the quark parton structure of nucleons has been collected since the pioneering experiment at SLAC which showed the first evidence of nucleon partonic substructure [1]. However, significantly less is known about the structure of other baryons. This is because of the impossibility of producing targets of short lived baryons for lepton nucleon deep-inelastic scattering (DIS) experiments which might measure their unpolarized or polarized structure functions. One possibility is to measure the fragmentation functions of quarks into baryons and relate the information obtained in these experiments to the quark structure of baryons. The Lambda hyperon is of special interest in this respect since its decay is self-analyzing. Polarization measurements are thus relatively simple to perform and the polarized fragmentation functions of quarks into  $\Lambda$  can be measured. Furthermore, in the quark parton model the  $\Lambda$  has a rather simple structure: the  $u$  and  $d$  quarks couple to a spin and an isospin singlet state, so the  $\Lambda$  spin is carried exclusively by its strange quark.

As is well known, the naive quark model fails to explain the data on hyperon  $\beta$  decay and on deep inelastic scattering [2–5]. The violation of the Ellis-Jaffe sum rule [6] suggests a large strange quark polarization in the nucleon. These observations suggest that the non-strange quarks of the  $\Lambda$  might also be substantially polarized [7]. This and related questions, together with the experimental feasibility of  $\Lambda$  polarization experiments, have stimulated much theoretical activity [7–34] on this subject. Information on the structure of the  $\Lambda$  should lead eventually to a deeper understanding of the structure of the nucleon.

In this paper, we re-examine assumptions such as  $SU(3)$

flavor and  $SU(6)$  spin-flavor symmetry, which are frequently crucial elements in predictions of  $\Lambda$  baryon structure. In Sec. II we point out that one should expect both the unpolarized and polarized quark distributions in the Lambda to show substantial differences from predictions based on either  $SU(3)$  flavor or  $SU(6)$  spin-flavor symmetry. The same mechanism which is responsible for breaking the  $SU(6)$  symmetry of the nucleon's quark distributions leads to  $x$ -dependent, polarized, non-strange valence quark distributions in the  $\Lambda$ . This contrasts with the naive expectation that the up and down valence quarks of the  $\Lambda$  should be unpolarized. In order to estimate the magnitude of these symmetry breaking effects and the size of the up and down quark polarizations, the quark distributions in the  $\Lambda$  are calculated in the MIT bag model. In Sec. III, we discuss how these flavor symmetry breaking effects carry over into the fragmentation of quarks into  $\Lambda$  baryons. In Sec. IV A, we show that the calculated fragmentation functions give a good overall description of all measured observables in inclusive particle production in  $e^+e^-$  annihilation. We also discuss the relevance of our approach to the dependence of the maximum of the  $\xi = \ln(1/z)$  spectrum on the mass of the produced particles. In Sec. IV B it is demonstrated that these polarized non-strange quark distributions give rise to sizable  $\Lambda$  polarization in polarized semi-inclusive DIS experiments, in contrast to predictions based on  $SU(3)$  flavor symmetry.

### II. QUARK DISTRIBUTIONS IN THE $\Lambda$

Baryon flavor symmetry is widely used to relate the structure of particles within the baryon octet. Flavor symmetry breaking effects are generally accounted for by using different phenomenological masses for the strange quark than for

up and down quarks. However,  $SU(3)$  symmetry breaking can be much more subtle, as has been pointed out in Refs. [23,24]. In a world of exact  $SU(6)$  spin-flavor symmetry the up and down quark distributions should be identical. Experiments indicate that they are different from each other; for example, it is known that the ratio  $d(x)/u(x)$  drops rapidly below unity as  $x \rightarrow 1$ . The hyperfine interaction responsible for the splitting of the  $\Delta$ - $N$  masses gives a natural explanation for this observation [25–27]. It is not yet clear whether this ratio actually goes to zero at  $x=1$  or approaches the perturbative QCD (pQCD) limit of 0.2 [28,29], although the latter now seems favored [30,31]. If  $SU(3)$  flavor symmetry is used to relate the  $\Sigma^+$  quark distributions to those in the proton, one would predict an analogous large- $x$  behavior,  $s_\Sigma/u_\Sigma \rightarrow 0$  for  $x \rightarrow 1$ . However, as has been pointed out in Refs. [23,24], the hyperfine interaction responsible for the splitting of the  $\Sigma$ - $\Lambda$  masses predicts a behavior opposite to the  $SU(3)$  expectation. For this reason it is mandatory that we re-examine  $SU(3)$  symmetry arguments in the  $\Lambda$  case. This has been done partly in our previous paper on the quark distributions in the  $\Lambda$  [24] and in a quark diquark spectator model for the fragmentation functions in Ref. [32] and also for the quark distribution functions [33]. Here, we extend our earlier discussion to fragmentation, emphasizing the close relationship between distribution and fragmentation functions. Since the publication of our paper, Ref. [24], there have been discussions along similar lines by Ma *et al.* [34].

It is instructive to review how the QCD hyperfine interaction breaks  $SU(6)$  spin-flavor symmetry. The leading-twist quark distributions can be formally defined as [35,36]

$$q_\Gamma(x) = P^+ \int \frac{d\xi^-}{2\pi} e^{ixP^+\xi^-} \langle \Lambda; PS | \bar{\psi}(0) \Gamma \psi(\xi^-) | \Lambda; PS \rangle, \quad (1)$$

where  $\Gamma$  is a Dirac matrix,  $P$  and  $S$  are respectively the momentum and spin of the  $\Lambda$  and we defined  $P^\pm \equiv P^0 \pm P^3$ . Inserting a complete set of intermediate states, using the translation invariance of the matrix elements and the integral representation of the  $\delta$  function the twist-2, helicity projections,  $q^{\uparrow\downarrow}$ , are given by

$$q^{\uparrow\downarrow}(x) = 2P^+ \sum_n \delta[(1-x)P^+ - p_n^+] \times |\langle n; p_n | \psi_{\uparrow\downarrow}^\dagger(0) | \Lambda; PS_\parallel \rangle|^2. \quad (2)$$

Here,  $\psi_{\uparrow\downarrow}^\dagger = \frac{1}{2}(1 + \gamma_0 \gamma_3) \frac{1}{2}(1 \pm \gamma_5) \psi$  with  $P_+ = \frac{1}{2}(1 + \gamma_0 \gamma_3)$  and  $\Lambda_\pm = \frac{1}{2}(1 \pm \gamma_5)$  [ $= \frac{1}{2}(1 \mp \gamma_5)$ ] are the relevant light-cone helicity projection operators for quarks [antiquarks] and we defined  $\gamma^+ = \gamma^0 + \gamma^3$ .  $S_\parallel$  is the spin vector parallel to the target's three-momentum. Further, the states  $|n; p_n\rangle$  are intermediate states with mass  $M_n$  and form a complete set of states with  $p_n^+ = \sqrt{M_n^2 + \mathbf{p}_n^2} + p_{nz}$ . All states are normalized to  $(2\pi)^3 \delta(\mathbf{p} - \mathbf{p}')$ .  $q^{\uparrow\downarrow}$  can be interpreted as the probability to find a quark with the same or opposite helicity as the target hyperon.

The advantage of using Eq. (2) is that energy-momentum conservation is ensured so that the resulting quark distribu-

tions have correct support. This is guaranteed by Eq. (2) regardless of the approximation used for the states  $|n; \mathbf{p}_n\rangle$  and  $|\Lambda; PS\rangle$ . The quark operator  $\psi$  acts on the initial state  $|\Lambda; PS\rangle$ . It either destroys a quark, producing an intermediate two quark state, or it inserts an anti-quark into the target, producing a four quark intermediate state. The delta function implies that the contribution to the quark distribution arising from an intermediate state with mass  $M_n$  peaks at

$$x_{max} \approx (1 - M_n/M_\Lambda). \quad (3)$$

As a result, the shape of the quark distribution at large  $x$  is determined by the smallest mass  $M_n$  which can contribute to the particular distribution. Since the mass of the intermediate state, in general, depends on the flavor of the struck quark, this mass dependence translates into a flavor dependence of the quark distribution functions of the baryon. We also see that contributions from four-quark intermediate states peak at *negative*  $x$  values, since  $M_n > M$ , and are thus suppressed in the positive  $x$  region.

QCD color-magnetic effects lift the mass degeneracy between hadrons that differ only in the orientation of quark spins, such as  $N$  and  $\Delta$ . The interaction is repulsive if the spins are parallel, so that a pair of quarks in a spin-1 state (vector) has higher energy than a pair of quarks in a spin-0 state (scalar). The energy shift between scalar and vector diquarks produces the  $N$ - $\Delta$  mass splitting. The  $\vec{s}_i \cdot \vec{s}_j$  structure of the hyperfine interaction shifts the mass of the vector and scalar diquarks in the ratio 1:−3. From the experimental  $\Delta$ - $N$  mass difference, we conclude that the triplet diquark is heavier by 50 MeV than the diquark state without hyperfine interaction, while the singlet diquark is lighter by 150 MeV. The diquark masses which reproduce the  $N$  and  $\Delta$  masses are roughly  $m_s \approx 600$  MeV and  $m_v \approx 800$  MeV for the scalar and vector diquarks, respectively. Since the  $d$  quark in the proton is always accompanied by a vector diquark as opposed to the  $u$  quark which has a large probability to be accompanied by a scalar diquark, the  $u$ -quark distribution peaks at larger  $x$  values than the  $d$ -quark distribution. Using Eq. (3) with the scalar and vector diquark masses, one obtains quantitative predictions for the location of the peak in the  $u$  and  $d$  valence quark distributions.

The same arguments applied to the  $\Lambda$  and  $\Sigma$  mass splitting predict that the  $us$  vector diquark is heavier by  $\approx 30$  MeV, and the corresponding scalar diquark is lighter by  $\approx 90$  MeV, than the diquark without hyperfine splitting. To estimate the masses of diquarks containing a strange quark and an up or down quark we use the phenomenological fact that the strange quark adds about 180 MeV. Thus, we have  $m'_s = 800 + 180 - 90 \approx 890$  MeV and  $m'_v = 800 + 180 + 30 = 1010$  MeV for singlet and triplet diquarks.

If the struck quark is accompanied by a scalar (vector) diquark, its distribution peaks at higher (lower)  $x$  values. The probabilities for finding a  $u$ ,  $d$  or  $s$  quark polarized parallel or anti-parallel to a  $\Lambda$  hyperon, and accompanied by a scalar or vector diquark, can be obtained from the  $SU(6)$  wave function of the  $\Lambda$  and are given in Table I. If the struck quark is a strange quark, the intermediate state must always be a scalar diquark; Eq. (3) shows that this will produce a very hard

TABLE I. The probabilities for finding a quark polarized parallel ( $\uparrow$ ) or anti-parallel ( $\downarrow$ ) to the Lambda and accompanied by a scalar ( $s$ ) or vector ( $v$ ) diquark.

$q(qq)_v$	$P[q(qq)_v]$	$q(qq)_s$	$P[q(qq)_s]$
$u_v^\uparrow = d_v^\uparrow$	1/12	$u_s^\uparrow = d_s^\uparrow$	1/12
$u_v^\downarrow = d_v^\downarrow$	2/12	$u_s^\downarrow = d_s^\downarrow$	0
$s_v^\uparrow$	0	$s_s^\uparrow$	4/12
$s_v^\downarrow$	0	$s_s^\downarrow$	0
net	1/2	net	1/2

strange quark distribution in the  $\Lambda$ . However, if the struck quark is an up or down quark, the remaining diquark has a higher probability to be a vector diquark than a scalar diquark. This leads to softer up and down quark distributions.

Furthermore, while the valence  $u_v$  or  $d_v$  quarks with spin anti-parallel to the  $\Lambda$  spin are always associated with a vector diquark,  $u_v$  and  $d_v$  quarks with spin parallel to the  $\Lambda$  spin have equal probabilities to be accompanied by a vector or scalar diquark. This has the important consequence that the distribution of non-strange quarks with spin parallel to the  $\Lambda$  spin is harder than the corresponding distributions with anti-parallel spins. Thus,  $u_v^\uparrow(x)$  [ $d_v^\uparrow(x)$ ] and  $u_v^\downarrow(x)$  [ $d_v^\downarrow(x)$ ] are shifted in  $x$  relative to each other, so that  $\Delta u_v(x) \equiv u_v^\uparrow(x) - u_v^\downarrow(x)$  and  $\Delta d_v(x) \equiv d_v^\uparrow(x) - d_v^\downarrow(x)$  are non-vanishing functions of  $x$ . They are positive for large  $x$  and negative for small  $x$  values. Note that their total contribution to the spin of the  $\Lambda$  is zero since the integrals over  $\Delta u_v$  and  $\Delta d_v$  are zero. Nevertheless,  $\Delta u_v$  and  $\Delta d_v$  can be sizable for large  $x$  values since both  $u_v$  and  $\Delta u_v$  are dominated by the spin-zero component in the large  $x$  limit.

These properties of the quark distributions are quite general. Once we assume that the intermediate states can be regarded as on shell physical states with definite masses, they follow immediately from the definition of the quark distributions and from the  $SU(6)$  structure of the baryon wave functions. Since, up to now, quark distributions cannot be calculated from first principles, we have to use model wave functions to estimate the magnitude of the expected symmetry breaking effects. We use MIT bag wave functions and the Peierls-Yoccoz method for constructing translationally invariant momentum eigenstates,  $|B_{\{n\}}\mathbf{p}\rangle$ , from  $n$  particle bag states  $|B_{\{n\}}(\mathbf{r})\rangle$ , centered at  $\mathbf{r}$ :

$$|B_{\{n\}}\mathbf{p}\rangle = [\phi_n(\mathbf{p})]^{-1} \int d\mathbf{r} e^{i\mathbf{p}\cdot\mathbf{r}} |B_{\{n\}}(\mathbf{r})\rangle. \quad (4)$$

The normalization  $\phi_n(\mathbf{p})$  is given by

$$|\phi_n(\mathbf{p})|^2 = \int d\mathbf{R} e^{-i\mathbf{p}\cdot\mathbf{R}} \langle B_{\{n\}}(\mathbf{R}) | B_{\{n\}}(\mathbf{0}) \rangle. \quad (5)$$

The matrix element in the definitions of the quark distribution functions can be obtained by using these bag states and the bag operator  $\psi = \sum_m \{b_m \psi_m(+)+d_m^\dagger \psi(-)\}$  [ $\psi_m(\pm)$  are the positive and negative energy solutions of the Dirac equa-

tion in the bag and  $b_m$ ,  $d_m^\dagger$  are annihilation and creation operators]. The spin-dependent parton distributions are then given by [37,38]

$$q_f^{\uparrow\downarrow}(x) = \frac{2M_\Lambda}{(2\pi)^2} \sum_m \langle \Lambda^\uparrow | P_{f,m} | \Lambda^\uparrow \rangle \times \int_{|M_\Lambda^2(1-x)^2 - M_n^2|/2M_\Lambda(1-x)}^\infty p_n d p_n \frac{|\phi_2(\mathbf{p}_n)|^2}{|\phi_3(\mathbf{0})|^2} \times |\psi_m^{\uparrow\downarrow}(\mathbf{p}_n)|^2. \quad (6)$$

Here,  $\uparrow\downarrow$  indicates the helicity projections. The operator  $P_{f,m}$  projects out the appropriate spin and isospin quantum numbers from the  $SU(6)$  wave functions of the polarized target baryon. Its matrix elements are given in Table I.  $\psi_m^{\uparrow\downarrow}(\mathbf{p}_n)$  is the Fourier transform of the bag wave function with angular momentum component  $m$ , and may be split into spin dependent and spin independent parts:

$$|\Psi_m^{\uparrow\downarrow}(\mathbf{p}_n)|^2 = \frac{1}{2} [f(\mathbf{p}_n) \pm (-1)^{m+3/2} g(\mathbf{p}_n)]. \quad (7)$$

Denoting by  $F(x)$  and  $G(x)$  those contributions to Eq. (6) which come from the  $f(\mathbf{p}_n)$  and  $g(\mathbf{p}_n)$  parts of the integral we obtain, for the unpolarized distributions,

$$d_\Lambda(x) = u_\Lambda(x) = \frac{1}{4} [3F_v(x) + F_s(x)]$$

$$s_\Lambda(x) = F_s(x), \quad (8)$$

and for the polarized quark distribution functions,  $\Delta q \equiv q^\uparrow - q^\downarrow$ ,

$$\Delta d_\Lambda(x) = \Delta u_\Lambda(x) = \frac{1}{4} [G_s(x) - G_v(x)]$$

$$\Delta s_\Lambda(x) = G_s(x), \quad (9)$$

respectively (see Refs. [37,38] for details of the proton case and Ref. [24] for other baryons).

The calculated quark distributions for the  $\Lambda$  are shown in Figs. 1 and 2 at the scale relevant for the bag model,  $\mu^2 = 0.25 \text{ GeV}^2$ , and with a bag radius of 0.8 fm. The distributions are compared to the corresponding quark distributions in the proton which were also calculated in the bag model, using the scalar and vector diquark mass splitting fixed from the  $\Delta$ - $N$  splitting. We see that the quark distributions of the  $\Lambda$  are quite different from  $SU(3)$  expectations,  $s_\Lambda \neq d_p$ , etc. Perfect  $SU(6)$  symmetry would give identical up, down and strange distributions. The strange quark distribution is much harder than the up and down quark distributions. The polarized up and down distributions are positive for large  $x$ . The non-strange distributions can play an important role whenever the strange contribution is suppressed, such as in processes induced by photons, where the up quark distributions

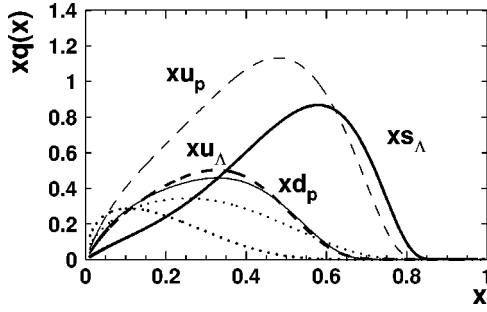


FIG. 1. Unpolarized quark distributions in the  $\Lambda$  (heavy lines) compared to those in the proton (light lines) at the bag scale,  $\mu^2$ . The quark distributions of the  $\Lambda$  evolved to  $Q^2=10 \text{ GeV}^2$  are shown as dotted lines.

are weighted by a factor of 4/9 as opposed to 1/9 for the strange quarks. Their relative magnitude is sizable as can be seen in Fig. 2, where we show five times  $x\Delta u(x)$  as a dotted line to indicate the relative contribution of  $u$  and  $d$  to  $g_1^\Lambda$ .

If the flavor dependence predicted for the polarization of non-strange quarks was retained in quark fragmentation, our predictions could be tested in semi-inclusive DIS experiments with longitudinally polarized electrons. Here, the smallness of the  $u$  and  $d$  polarizations relative to the strange quark polarization is compensated by the abundance of  $u$  quarks in the valence region, and by the enhancement factor of 4/9 for the  $u$  quark (relative to the factor 1/9 for  $s$  quarks) in electro-magnetic interactions [39].  $\Lambda$ 's produced in the current fragmentation region are mainly fragmentation products of  $u$  quarks. Part of the polarization of the electron is transferred to the struck quark in the scattering process. This polarization will be transferred to the final  $\Lambda$  if the helicity dependent fragmentation functions,  $\Delta D_u^\Lambda$ , are non-zero [39]. In the following section we extend our discussion to fragmentation and compare the resulting predictions with experimental data on hyperon formation and polarization and with predictions of other models for the fragmentation functions.

### III. QUARK FRAGMENTATION INTO $\Lambda$ HYPERONS

Since the quark distributions of the  $\Lambda$  baryon are not flavor symmetric, it is probable that the quark fragmentation

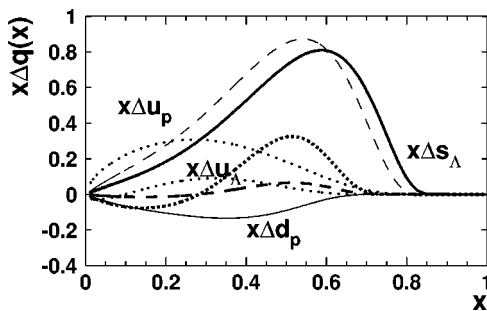


FIG. 2. Polarized quark distributions in the  $\Lambda$  (heavy lines) compared to those in the proton (light lines) at the bag scale,  $\mu^2$ . The heavy dotted line stands for 5 times  $x\Delta u_\Lambda$  and indicates the relative importance of the  $u$  and  $d$  quarks in  $g_1^\Lambda$ . The quark distributions of the  $\Lambda$  evolved to  $Q^2=10 \text{ GeV}^2$  are shown as dotted lines.

functions are also flavor asymmetric. In the fragmentation of quarks into a specific baryon, quarks with different flavor couple to different spin-flavor components of the baryon wave function. For example, in order to produce a  $\Lambda$  from an up (down) quark or a strange quark, the fragmentation process has to produce a  $ds$  ( $us$ ) vector or  $ud$  scalar diquark. The mass differences between the scalar and vector diquarks inevitably lead to flavor dependent fragmentation functions, analogous to the flavor dependence of the quark distributions.

Fragmentation functions can be defined in a manner similar to quark distribution functions, as light-cone Fourier transforms of matrix elements of quark operators [35,40]:

$$\begin{aligned} \frac{1}{z} D_{q\Lambda}^\Gamma(z) &= \frac{P^+}{2} \sum_n \int \frac{d\xi^-}{2\pi} e^{-iP^+\xi^-/z} \\ &\times \text{Tr}\{\Gamma \langle 0 | \psi(0) | \Lambda(PS); n(p_n) \rangle \\ &\times \langle \Lambda(PS); n(p_n) | \bar{\psi}(\xi^-) | 0 \rangle\}, \end{aligned} \quad (10)$$

Here,  $\Gamma$  is the appropriate Dirac matrix. Translating the matrix elements, using the integral representation of the delta function and projecting out the light-cone helicity components, we obtain

$$\begin{aligned} \frac{1}{z} D_{q\Lambda}^{\uparrow\downarrow}(z) &= P^+ \sum_n \delta[(1/z-1)P^+ - p_n^+] \\ &\times |\langle 0 | \psi_{\uparrow\downarrow}^\dagger(0) | \Lambda(PS_{\parallel}); n(p_n) \rangle|^2. \end{aligned} \quad (11)$$

$D_{q\Lambda}^{\uparrow\downarrow}$  can be interpreted as the probability that a right- or left-handed quark fragments into a right-handed  $\Lambda$  and similar for antiquarks. Using Eq. (11) has the advantage that energy-momentum conservation is built in *before* any approximation is made for the states in the matrix element. The delta function in Eq. (11) implies that the function  $D_{q\Lambda}/z$  peaks at

$$z_{max} \approx \frac{M_\Lambda}{M_\Lambda + M_n}, \quad (12)$$

where we have chosen to work in the rest frame of the  $\Lambda$ . For  $M_n=2/3M_\Lambda$  and  $M_n=4/3M_\Lambda$ , we obtain 3/5 and 3/7, respectively. The contributions from the four quark intermediate states therefore peak in the physical region, at relatively large  $z$  values. Thus, in contrast to the quark distribution functions, the fragmentation functions are not dominated by the lowest intermediate mass states. However, we still expect that for large  $z$  the most important contribution comes from the fragmentation of a quark into a  $\Lambda$  and a diquark state. Since the fragmentation functions are sensitive to the mass of the intermediate states, our arguments on  $SU(6)$  flavor symmetry breaking apply in the same way to the fragmentation functions as to the quark distributions. Most importantly, since  $u^\uparrow$  and  $u^\downarrow$  couple to different spin-flavor components of the Lambda wave function, we expect that not only are the  $u$  and  $d$  quarks in a polarized  $\Lambda$  hyperon polarized, but that  $u$  and  $d$  quarks may also fragment into a polarized  $\Lambda$ . Furthermore,  $\Delta D_{u\Lambda}$  and  $\Delta D_{d\Lambda}$  are positive at large  $z$  for the same



reason as  $\Delta u$  and  $\Delta d$  are positive at large  $x$ . Thus, for example,  $\Lambda$ 's produced in the current fragmentation region of semi-inclusive DIS processes should be positively polarized.

We stress that, as for the quark distributions, our analysis is very general and follows from the definition of the fragmentation functions and from energy momentum conservation. The matrix elements can be calculated using model wave functions at the scale relevant to the specific model and the resulting fragmentation functions can be evolved to a higher scale to compare them to experiments. First, let us discuss the action of the operators in Eq. (11). The operator,  $\psi_+$  ( $\psi_+^\dagger$  for antiquark fragmentation), when acting on the state  $\Lambda$  in the final state:

(i) Can destroy a quark in  $\Lambda$  leaving a diquark state which has to match the quantum numbers of the anti-diquark state to give vacuum quantum numbers. This corresponds to the fragmentation of the quark via production of two quark antiquark pairs from the vacuum  $q \rightarrow (qqq) + (\bar{q}\bar{q})$ , i.e. the fragmentation of  $q$  into a  $\Lambda$  and an anti-diquark.

(ii) Alternatively, it can insert quark or antiquark into the  $\Lambda$  wave function. In this case, the intermediate state must be a four-quark state such that vacuum quantum numbers are preserved. This corresponds to the fragmentation of an antiquark or quark into a  $\Lambda$  via production of three quark antiquark pairs,  $\bar{q} \rightarrow (qqq) + (\bar{q}\bar{q}\bar{q})$  or  $q \rightarrow (qqq) + (q\bar{q}\bar{q})$ .

In order to quantify our discussion we have to use model wave functions for the states. Choosing the Peierls-Yoccoz projection method and MIT bag wave functions, the fragmentation functions are given by

$$D_{f\Lambda}^{\uparrow\downarrow}(x) = \frac{zM_\Lambda}{(2\pi)^2} \sum_m \langle \Lambda^\uparrow | P_{f,m} | \Lambda^\uparrow \rangle \times \int_{p_{min}}^{\infty} p_n dp_n \langle 0 | \psi_+^{\uparrow\downarrow}(0) | \Lambda(PS_{\parallel}); n(p_n) \rangle^2. \quad (13)$$

with

$$p_{min} = \left| \frac{M_\Lambda^2(1-z)^2 - z^2 M_n^2}{2M_\Lambda z(1-z)} \right|. \quad (14)$$

The matrix element for the fragmentation through a diquark intermediate state yields

$$\begin{aligned} & \langle 0 | \psi_+^{\uparrow\downarrow}(0) | \Lambda(PS_{\parallel}); n(p_n) \rangle \\ &= [\phi_2(\mathbf{p}_n) \phi_3(\mathbf{0})]^{-1} \hat{\psi}_+^{\uparrow\downarrow}(-\mathbf{p}_n) \\ & \times \int d\mathbf{R} e^{i\mathbf{p}_n \cdot \mathbf{R}} \langle 0 | B_2(\mathbf{0}) B_{\bar{2}}(\mathbf{R}) \rangle. \end{aligned} \quad (15)$$

Here,  $\phi_2(\mathbf{p}_n)$  and  $\phi_3(0)$  are normalization constants of the final states.  $\hat{\psi}_+^{\uparrow\downarrow}(-\mathbf{p}_n)$  is the Fourier transform of the projected bag wave function. The matrix element,  $\langle 0 | B_2(\mathbf{0}) B_{\bar{2}}(\mathbf{R}) \rangle$ , describes the transition between the diquark and anti-diquark states and the vacuum. We assume that it is proportional to the overlap of the diquark and anti-diquark states with a  $\gamma_0$  sandwiched between them

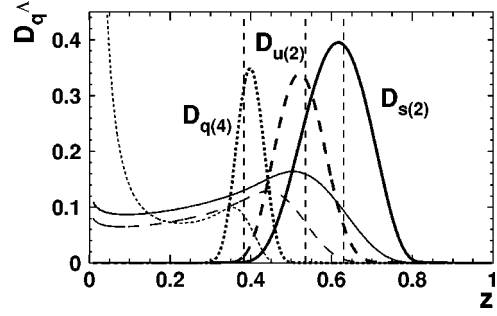


FIG. 3. Contributions of two and four quark intermediate states to the unpolarized fragmentation functions at the bag scale (heavy lines) and evolved to  $Q^2 = 10 \text{ GeV}^2$  (light lines). The mass of the four-quark intermediate state is set to 1.8 GeV and  $D_{q(4)}$  is a sum over flavors,  $D_{q(4)} = D_{\bar{u}\Lambda} + D_{\bar{d}\Lambda} + D_{\bar{s}\Lambda}$ . The dashed vertical lines indicate the position of the maxima using Eq. (12).

$\langle \bar{B}_{\bar{2}}(\mathbf{R}) | B_2(\mathbf{0}) \rangle$ .<sup>1</sup> We will calculate this overlap and adjust the normalization constant by fitting one data point later when we discuss the phenomenological implications of our fragmentation functions. The expression for the four quark intermediate states can be obtained by replacing  $\phi_2$ ,  $B_2$  and  $B_{\bar{2}}$  through  $\phi_4$ ,  $B_4$  and  $B_{\bar{4}}$  and by replacing the positive energy, ground state bag solutions,  $\hat{\psi}_{+1s}^{\uparrow\downarrow}(-\mathbf{p}_n)$  by  $\hat{\psi}_{+1s}^{\uparrow\downarrow}(\mathbf{p}_n)$  or by the corresponding negative energy state  $\hat{\psi}_{+1s}^{\uparrow\downarrow}(-\mathbf{p}_n)$  for the three anti-quark one quark intermediate state or the four anti-quark intermediate state, respectively [38].

Denoting by  $\hat{F}(z)$  and  $\hat{G}(z)$  those contributions to Eq. (13) which come from the  $f(-\mathbf{p}_n)$  and  $g(-\mathbf{p}_n)$  parts of the integral, the contributions from the diquark intermediate states to the fragmentation functions are then given by

$$D_{d\Lambda}(z) = D_{u\Lambda}(z) = \frac{1}{4} [3\hat{F}_v(z) + \hat{F}_s(z)]$$

$$D_{s\Lambda}(z) = \hat{F}_s(z)$$

$$\Delta D_{d\Lambda}(z) = \Delta D_{u\Lambda}(z) = \frac{1}{4} [\hat{G}_s(z) - \hat{G}_v(z)]$$

$$\Delta D_{s\Lambda}(z) = \hat{G}_s(z), \quad (16)$$

with  $\Delta D_{q\Lambda} \equiv D_{q\Lambda}^\uparrow - D_{q\Lambda}^\downarrow$ . Since  $\hat{G}_s$  is shifted towards positive  $z$  values relative to  $\hat{G}_v$ ,  $\Delta D_{d\Lambda}$  and  $\Delta D_{u\Lambda}$  are positive for large  $z$ . The results are shown in Figs. 3 and 4. We show the results both at the bag scale  $\mu^2 = 0.25 \text{ GeV}^2$  and at  $Q^2 = 10 \text{ GeV}^2$ . We evolved the fragmentation functions in leading order and set the gluon fragmentation function to zero at

<sup>1</sup>This factor is basically a normalization factor. In the case of the quark distributions, the corresponding expression gives just  $|\phi_2(\mathbf{p}_n)|^2$ . It has a small effect on the shape of the fragmentation functions which is mainly determined by the kinematic constraints and the Fourier transform of the wave function of the struck quark.

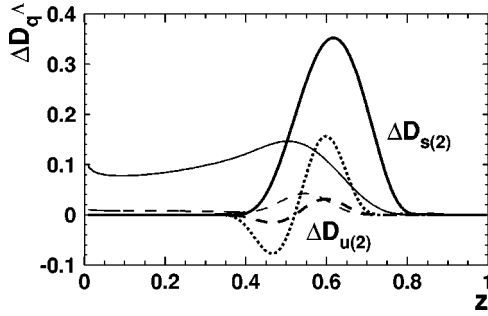


FIG. 4. Contributions of two quark intermediate states to the polarized fragmentation functions at the bag scale (heavy lines) and evolved to  $Q^2 = 10 \text{ GeV}^2$  (light lines). The dotted line stands for 5 times  $\Delta D_u^\Lambda$ .

the starting scale for non-singlet evolution. We used the package of Ref. [52] modified for the evolution of fragmentation functions.

The fragmentation functions possess the following qualitative features:

- (1) The mass splitting associated with the hyperfine interaction leads to considerable  $SU(6)$  breaking in the fragmentation functions.
- (2) At large  $z$ , fragmentation functions are dominated by the diquark intermediate states.
- (3) Since the contributions of higher mass states to fragmentation functions have maxima in the physical region, they play an important role at lower  $z$  values.
- (4) The splitting of the vector and scalar diquark masses leads to polarized, non-strange fragmentation functions.

#### IV. PHENOMENOLOGY

##### A. $e^+e^-$ annihilation at the $Z$ resonance

Before making predictions for the expected  $\Lambda$  polarization in semi-inclusive DIS, we check whether available  $\Lambda$  production data are consistent with our approach.

Let us start our discussion with an interesting consequence of our approach for the lower- $z$  end of the spectrum of particles produced in  $e^+e^-$  annihilation. When the number of particles produced is plotted as a function of  $\xi = \ln(1/z)$ , one finds that the spectra exhibit an approximate Gaussian shape around a maximum,  $\xi^*$ , which depends on the produced particle [41–44]. While the shape of the spectrum can be understood in perturbative QCD as a consequence of the coherence of gluon radiation [45], the position of the maximum is a free parameter which has to be extracted from experiment. Energy-momentum conservation dictates that the spectrum at small  $z$  be dominated by high mass intermediate states. At a given total invariant mass  $\sqrt{s}$ , there will be a maximum value for the mass of the intermediate state which can be produced in the fragmentation. This maximal mass determines the “lower” edge of the spectrum. Note also that because of the  $1/z$  factor in the lower limit of the integration in Eq. (13), the fragmentation function drops at low  $z$  values. The  $\xi$  distribution is given by  $d\sigma/d\xi = z d\sigma/dz \sim z D(z)$ , and thus it is proportional to  $z^2$  times  $D(z)/z$ . Although Eq. (12) describes the location of the

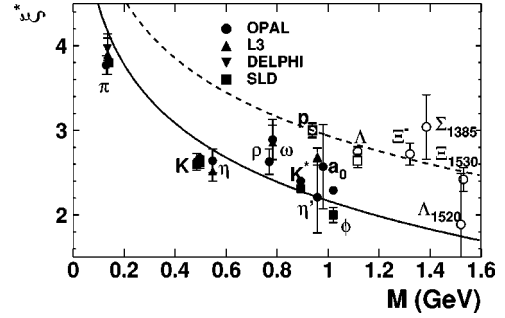


FIG. 5. Location of the maxima of the  $\xi$  distributions as a function of the particle mass. The solid and open symbols represent mesons and baryons, respectively. The data are from [41–44]. The solid and dashed lines are the prediction of Eq. (17) for mesons and baryons, adjusting the normalization to  $\xi_{\eta'}$ , and to  $\xi_p^*$ , respectively.

maxima of the distribution  $D(z)/z$ , we can expect that Eq. (12) is also a good approximation for the  $\xi$  distribution since the fragmentation functions for a given mass  $M_n$  are very narrow, as can be seen in Fig. 3.

From Fig. 3, we can also see that Eq. (12) is a good approximation for the maximum of  $D(z)$ . [Equation (12) gives the maximum of the  $\xi$  distribution exactly in the limit when the distribution is a  $\delta$  function.] In the following, we will use Eq. (12) to estimate the maxima of the  $\xi$ -distribution. Now, the maximum of the distribution coming from this highest mass state determines the maximum of the fragmentation function in first approximation through Eq. (12). Although  $M_n$  is not known, it should be proportional to  $\sqrt{s}$ . Thus, the maximum of the  $\xi$  distribution has the correct  $\ln(s)$  dependence as seen in the experiment [41–44]. However, if we take the difference of the maxima of the  $\xi = \ln(1/z)$  distributions of different particles, this dependence on the unknown maximum value of  $M_n$  drops out for large  $M_n$ . It follows from Eq. (12) that

$$\Delta \xi^* = \xi_a^* - \xi_b^* \approx \ln\left(\frac{M_a + M_n}{M_b + M_n}\right) + \ln\frac{M_b}{M_a} \approx \ln\frac{M_b}{M_a}. \quad (17)$$

Thus, the difference of the maxima is determined by the logarithm of the ratio of the masses. We calculated the maxima of the  $\xi$  distributions using this formula and taking the maximum of the  $\eta'$  and the proton distributions as a reference value for mesons and baryons, respectively. The results are compared to the experimental data [41–44] in Fig. 5. We stress that our results follow from the general definition of the fragmentation functions and from energy-momentum conservation and are in remarkably good agreement with the data.

Let us turn our attention to the high  $z$  region where, according to our discussion in Sec. II, significant flavor symmetry breaking effects are to be expected. There are experimental data for the production of  $\Lambda$  hyperons in  $e^+e^-$  annihilation. A considerable fraction of the data was taken at the  $Z$  resonance, where the quarks produced in the annihilation process are longitudinally polarized. The spin dependent fragmentation functions can then be determined by measuring the polarization of the produced Lambda baryons.

In the quark parton model, the cross section for the inclusive production of a Lambda hyperon,  $e^+e^- \rightarrow \Lambda + X$ , is obtained by summing over the cross sections for  $e^+e^- \rightarrow q\bar{q}$  and weighting with the probabilities  $D_{q\Lambda}$  that a quark fragments into a Lambda with energy fraction  $z$ :

$$\frac{d^2\sigma_\Lambda}{dzd\Omega} = \sum_q \frac{d\sigma^q}{d\Omega} [D_{q\Lambda}(z, Q^2) + D_{\bar{q}\Lambda}(z, Q^2)]. \quad (18)$$

Here,  $z$  is defined as  $z = 2p_\Lambda \cdot q / Q^2 = 2E_\Lambda / \sqrt{s}$  for center-of-mass system (c.m.s.) energy  $\sqrt{s}$ , and  $p_\Lambda$  and  $E_\Lambda$  are the four-momentum and energy of the  $\Lambda$ ;  $q$  and  $Q^2 \equiv q^2 = s$  are respectively the four-momentum and invariant mass of the virtual  $Z$  boson.

After integrating over angles, the cross section at the  $Z$  resonance can be written as

$$\frac{d\sigma_\Lambda}{dz} = \frac{4\pi\alpha^2}{s} \sum_q \hat{e}_q^2 [D_{q\Lambda}(z, Q^2) + D_{\bar{q}\Lambda}(z, Q^2)], \quad (19)$$

where the coupling of the quarks is given by

$$\hat{e}_q^2 = e_q^2 + (1 + v_e^2)(1 + v_q^2)\chi(M_Z^2)$$

with

$$\chi(s) = \frac{1}{256 \sin^4 \Theta_W \cos^4 \Theta_W} \frac{s^2}{(s - M_Z^2)^2 + \Gamma_Z^2 M_Z^2}, \quad (20)$$

where  $M_Z$  and  $\Gamma_Z$  are the mass and width of the  $Z$ .  $v_e = -1 + 4 \sin^2 \Theta_W$ ,  $v_u = 1 - \frac{8}{3} \sin^2 \Theta_W$ ,  $v_d = -1 + \frac{4}{3} \sin^2 \Theta_W$  are the vector coupling of the electron and the quarks to the  $Z$ .<sup>2</sup>

In the following, we introduce ‘‘valence’’ and ‘‘sea’’ type fragmentation functions  $D_{q_v\Lambda} \equiv D_{q\Lambda} - D_{\bar{q}\Lambda}$ , and  $D_{q_s\Lambda} \equiv D_{\bar{q}\Lambda}$ . Equation (19) can then be re-written as

$$\frac{d\sigma_\Lambda}{dz} = \frac{4\pi\alpha^2}{s} \sum_q \hat{e}_q^2 [D_{q_v\Lambda}(z, Q^2) + 2D_{q_s\Lambda}(z, Q^2)]. \quad (21)$$

Experimental measurements show that the particles produced containing the initial quark as a valence quark have higher momenta than the other hadrons in the jet—this is the ‘‘leading particle’’ effect. For example,  $\Lambda$ 's produced in a light quark jet have higher momenta than  $\bar{\Lambda}$ , indicating that the fragmentation functions  $D_{q\Lambda}$  are harder than  $D_{q\bar{\Lambda}}$ , or by  $CP$  invariance harder than  $D_{\bar{q}\Lambda}$ . Thus, the flavor non-singlet combination of the fragmentation functions,  $D_{q_v\Lambda} \equiv D_{q\Lambda} - D_{\bar{q}\Lambda}$ , effectively measures leading particle production and can be identified with the contribution from the diquark component of the fragmentation functions, for obvious reasons. On the other hand, particles produced in the fragmentation

<sup>2</sup>Since the data are taken at the  $Z$ -resonance peak, we have dropped terms in Eq. (19) which cancel for  $s = M_Z^2$ . Note also that the terms proportional to  $e_q^2$  are very small and can be neglected in numerical calculations.

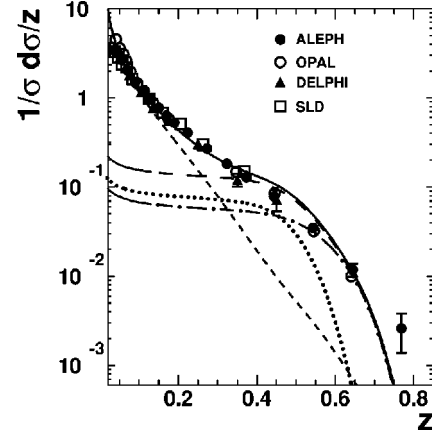


FIG. 6. The inclusive cross section  $(1/\sigma_{tot})d\sigma^\Lambda/dz$  in  $e^+e^-$  annihilation at the  $Z$  resonance. The dash-dotted and the dotted lines represent the contributions from  $D_{s_v}$  and  $D_{u_v} + D_{d_v}$ , respectively; the dashed line is the total  $D_{q_v}$  contribution and the short dashed line stands for  $D_{q_s}$ . The data are from Refs. [46–49,44].

process populate more the central rapidity region and are likely to be independent of the flavor of the initial quarks. Thus, the ‘‘sea’’ type fragmentation functions  $D_{q_s\Lambda} \equiv D_{\bar{q}\Lambda}$  can be identified with the contributions from intermediate four quark higher mass states.

In the following, we use our calculated fragmentation functions for the valence contribution and parametrize the sea part, since the mass of the higher mass four quark states is not well known. As the production of non-leading particles is independent of the flavor of the initial quarks, it is reasonable to assume that the sea type fragmentation functions are flavor symmetric—i.e.  $D_{q_s\Lambda} \equiv D_{u_s\Lambda} = D_{\bar{u}\Lambda} = D_{d_s\Lambda} = \dots = D_{\bar{b}\Lambda}$ . As the  $e^+e^-$  experiments measure the sum of  $\Lambda$  and  $\bar{\Lambda}$  production [44,46–49], we use  $CP$  invariance to relate the fragmentation functions of the  $\Lambda$  to those of the  $\bar{\Lambda}$ , i.e.  $D_{q\Lambda} = D_{q\bar{\Lambda}}$  and  $D_{\bar{q}\Lambda} = D_{q\bar{\Lambda}}$ . We evolve the fragmentation functions in leading order  $Q^2$  evolution from the scale relevant to the bag model,  $\mu^2 = 0.25 \text{ GeV}^2$ , to  $M_Z^2$  in order to obtain  $D_{q_v\Lambda}(z, Q^2 = M_Z^2)$ . In order to evolve the singlet part of the fragmentation functions, we assume that the gluon fragmentation functions are zero at the starting scale. Our result is shown in Fig. 6 in comparison with data from SLAC Large Detector (SLD) [44] and the CERN  $e^+e^-$  collider LEP experiments [46–49]. The long dashed line represents the contribution of  $D_{q_v}$ , the dotted line is the fitted sea quark fragmentation  $D_{q_s}$  and the solid line is the sum of the two contributions. The dash-dotted and short dashed lines are the contributions of strange and up plus down valence terms, respectively. We do not attempt to reproduce the data at low  $z$  values where gluon coherence effects become important and the usual evolution equations [50,51] break down [45]. The data clearly favor a two component picture.

The asymmetry in leading and non-leading particle production in  $e^+e^-$  annihilation provides a further test for the fragmentation functions. This asymmetry has been measured by the SLD Collaboration [44] and is defined as

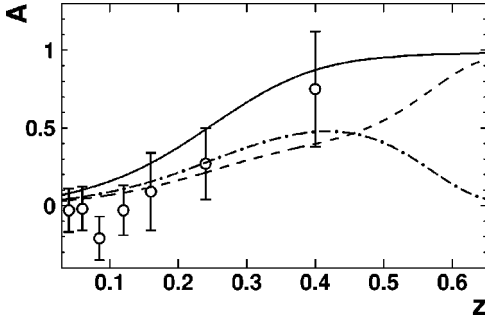


FIG. 7. The asymmetry between leading and non-leading lambda production. The solid line is the prediction of the two component picture. The dashed and dash-dotted lines are the contributions from the strange and from the up plus down quarks, respectively. The data are taken from Ref. [44].

$$A = \frac{R_{\Lambda}^q - R_{\bar{\Lambda}}^q}{R_{\Lambda}^q + R_{\bar{\Lambda}}^q} \quad (22)$$

with

$$R_{\Lambda}^q = \frac{1}{2N_{ev}} \frac{d}{dz} [N(q \rightarrow \Lambda) + N(\bar{q} \rightarrow \bar{\Lambda})]$$

$$R_{\bar{\Lambda}}^q = \frac{1}{2N_{ev}} \frac{d}{dz} [N(q \rightarrow \bar{\Lambda}) + N(\bar{q} \rightarrow \Lambda)] \quad (23)$$

where  $dN[q(\bar{q}) \rightarrow \Lambda(\bar{\Lambda})]/dz$  is the number density of  $\Lambda$ 's ( $\bar{\Lambda}$ 's) produced in a  $q$  ( $\bar{q}$ ) jet normalized to the total number of events  $N_{ev}$ . While a zero value of the asymmetry corresponds to equal production of hadrons and anti-hadrons, a value of +1 (-1) corresponds to total dominance of hadron (anti-hadron) production. In our model, the asymmetry is given by

$$A = \frac{\sum_q \hat{e}_q^2 D_{q_v\Lambda}(z, Q^2)}{\sum_q \hat{e}_q^2 [D_{q_v\Lambda}(z, Q^2) + 2D_{q_s\Lambda}(z, Q^2)]}. \quad (24)$$

Here, the summation runs only over the light flavors since only light quark jets were used in the experimental determination of the asymmetry. Our results are compared to the data in Fig. 7. The dashed and dash-dotted lines are the strange quark and up plus down quark contributions, and the solid line is their sum. Our model gives reasonable agreement with  $A$  as measured by SLD. At high  $z$ , the initial strange quarks give the dominant leading particle contribution to the asymmetry.

Unpolarized  $e^+e^-$  cross section measurements clearly support a two component picture of quark fragmentation. However, they cannot differentiate between a flavor symmetric model and a flavor asymmetric picture for the fragmentation functions. For example, both the total cross section and the asymmetry between leading and non-leading particle production could be described in a model with flavor sym-

metric fragmentation functions. Therefore, more information is needed to differentiate between the two models. Polarization measurements at the  $Z$  resonance can give additional constraints on the fragmentation functions.

The initial quarks produced in  $e^+e^-$  annihilation at the  $Z$  resonance are polarized because the parity violating coupling of the fermions favors certain helicity states. This initial polarization of the produced quarks can be transferred to the final state hadrons and may lead to polarized lambda production [7]. The difference between the cross sections to produce left- or right-handed lambdas at the  $Z$  resonance is given by [7]

$$\frac{d\Delta\sigma}{dz} \equiv \frac{d\sigma_L}{dz} - \frac{d\sigma_R}{dz}$$

$$= \frac{4\pi\alpha^2}{s} \sum_q \hat{g}_q [\Delta D_{q\Lambda}(z, Q^2) - \Delta D_{\bar{q}\Lambda}(z, Q^2)], \quad (25)$$

with the effective couplings

$$\hat{g}_q = 2a_q v_q (1 + v_e^2) \chi(M_Z^2). \quad (26)$$

Here,  $a_u = -a_d = 1$  are the axial vector coupling of the quarks to the  $Z$  and  $\chi$  was defined in Eq. (20). We introduce valence and sea type polarized fragmentation functions  $\Delta D_{q_v\Lambda} \equiv \Delta D_{q\Lambda} - \Delta D_{\bar{q}\Lambda}$  and  $\Delta D_{q_s\Lambda} \equiv \Delta D_{\bar{q}\Lambda}$  similar to the unpolarized case. According to our interpretation, the valence type fragmentation functions are given by the fragmentation of quarks into a  $\Lambda$  and an anti-diquark.

Since the hyperfine interaction leads to polarized up and down quark distributions for the lambda, we expect that polarized up and down quarks may also fragment into polarized  $\Lambda$ 's. On the other hand,  $\Delta D_{q_s\Lambda}$  is given by the contributions of four quark states. Since these are insensitive to the  $SU(6)$  wave function of the  $\Lambda$ , we expect that they do not contribute to polarized lambda production. Note that since the difference of the cross sections in Eq. (25) is proportional only to the valence part of the polarized fragmentation functions, the former assumption is not necessary for the description of the cross section difference.

The calculated lambda polarization,  $P_{\Lambda} = -\Delta\sigma/\sigma$ , is compared to the Aleph [53] and OPAL data [54] in Fig. 8. The dominant contribution comes from the fragmentation of strange quarks (the dash-dotted curve in Fig. 7). The contribution from up and down quarks (dashed curve) is negligible because the corresponding polarized valence type fragmentation functions are small. The non-strange quark contribution to the  $\Lambda$  polarization also peaks at lower  $z$  values where non-leading particle production dominates. In the limit  $z \rightarrow 1$ , both  $\Delta\sigma$  and  $\sigma$  are dominated by strange quark fragmentation and  $P_{\Lambda}$  behaves like

$$\lim_{z \rightarrow 1} P_{\Lambda}(z) = \frac{2v_d}{(1+v_d^2)} \frac{\Delta D_{s_v\Lambda}}{D_{s_v\Lambda}} \approx -0.94 \frac{\Delta D_{s_v}^{\Lambda}}{D_{s_v\Lambda}}, \quad (27)$$



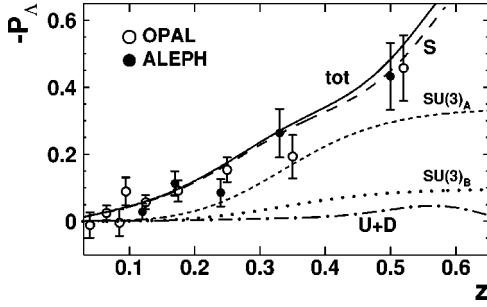


FIG. 8. Lambda polarization in  $e^+e^-$  annihilation at the Z resonance. The solid line is the prediction of the two component picture. The dashed and dash-dotted lines are the contributions from the strange and from the up plus down quarks. The short dashed and dotted lines correspond to the prediction of a model with flavor symmetric fragmentation functions using the naive quark parton model [ $SU(3)_A$ ] and  $g_1$  measurements for the proton plus  $SU(3)$  flavor symmetry to relate the polarized fragmentation functions to the unpolarized ones [ $SU(3)_B$ ]. The data are taken from Refs. [53,54].

where we have used  $\sin^2 \theta_W \approx 0.23$ . Since  $\Delta D_{s_{v\Lambda}} \rightarrow D_{s_{v\Lambda}}$  in the limit  $z \rightarrow 1$ ,  $P_\Lambda(z)$  approaches  $-0.94$  for  $z \rightarrow 1$ . In deriving Eq. (27), we neglected the production of higher mass hyperons and their subsequent decays into  $\Lambda$ . If these hyperons are produced by the initial quarks they are, in general, also polarized and can transfer part of their polarization to the final  $\Lambda$ . However, the distribution of the  $\Lambda$ 's coming from the decays of such hyperons should be shifted towards smaller  $z$  values, where the contribution from the  $q_{s\Lambda}$  is large and this will strongly suppress any polarization.<sup>3</sup>

We can contrast our predictions with those from models with flavor symmetric fragmentation functions. We set  $D_{s\Lambda} = D_{u\Lambda} = D_{d\Lambda}$  and discuss two different scenarios proposed in the literature [7,17,18] for the spin dependent fragmentation functions:<sup>4</sup>

(A) Naive quark model inspired scenario: all spin dependent fragmentation functions except for  $\Delta D_{s\Lambda}$  are zero.

(B) Predictions based on  $SU(3)$  flavor symmetry and polarized DIS on nucleon targets: not only the  $\Delta D_{s\Lambda}$  but also  $\Delta D_{u\Lambda}$  and  $\Delta D_{d\Lambda}$  are non-vanishing.

In both cases, we set the polarized valence type fragmentation functions proportional to the unpolarized ones:

$$\Delta D_{s\Lambda}(z) = c_s D_{s\Lambda}(z), \quad \Delta D_{u\Lambda}(z) = \Delta D_{d\Lambda}(z) = c_u D_{u\Lambda}(z). \quad (28)$$

In case (A), we have  $c_s = 1$  and  $c_u = 0$ , and in case (B), we have  $c_s = 0.6$  and  $c_u = -0.2$ . We could allow a different  $z$  dependence between the polarized and unpolarized quark distributions by multiplying by a power of  $z$ , for example. However, we are interested in the upper limits one can obtain from flavor symmetric models. Since the polarized fragmen-

<sup>3</sup>For a discussion of the effect of hyperon decays on the  $\Lambda$  polarization see Refs. [11,19].

<sup>4</sup>See Ref. [18] for a next to leading order analysis along the same lines.

tion functions are bounded by the positivity constraint,  $|\Delta D_q| \leq D_q$ , we have not included a suppression factor.

The limiting behavior of the polarization is

$$\lim_{z \rightarrow 1} P_\Lambda^{(A)}(z) = \frac{2v_d}{(1+v_u^2) + 2(1+v_d^2)} \approx -0.34$$

$$\lim_{z \rightarrow 1} P_\Lambda^{(B)}(z) = \frac{2[(c_u + c_s)v_d - c_u v_u]}{(1+v_u^2) + 2(1+v_d^2)} \approx -0.1, \quad (29)$$

for cases (A) and (B), respectively. The unpolarized cross sections were fit using flavor symmetric fragmentation functions for both the valence and sea type fragmentation functions, and the lambda polarization was calculated using Eq. (28). The results are shown in Fig. 8. Even when the positivity constraint is saturated, i.e.  $\Delta D_{s\Lambda} = D_{s\Lambda}$ , the lambda polarization for high  $z$  values is considerably smaller than experiment in both cases. The data strongly suggest that the fragmentation functions cannot be flavor symmetric.

In this connection, we note that Monte Carlo models often used by the experimental Collaborations, e.g. JETSET [55] which is based on the Lund fragmentation model [56], can describe the  $P_\Lambda$  data using parameters obtained from the naive quark model for the  $\Lambda$  spin content. However, these Monte Carlo programs have built in parameters which suppress

- (a) the production of strange quarks relative to up and down quarks,
- (b) the production of strange diquarks relative to diquarks containing only up and down quarks, and
- (c) the production of vector diquarks relative to scalar diquarks.

These suppression factors result in *flavor asymmetric* fragmentation functions. For example, an initial strange quark has a higher probability to fragment into a lambda than an up or down quark, due to the suppression for the production of strange diquarks from the vacuum. The suppression factor (c) makes it straightforward to implement our ideas in a polarized version of such Monte Carlo programs.

## B. Semi-inclusive deep-inelastic scattering

We have seen that, in  $e^+e^-$  annihilation, a flavor separation of the polarized fragmentation function is not possible because the lambda polarization is dominated by the fragmentation of strange quarks. However, since fragmentation of up quarks is the dominant channel for lambda production in semi-inclusive DIS, this process is very useful for studying the polarized up quark distribution functions, as was pointed out in Ref. [39].

The lambda polarization resulting from the scattering of polarized electrons from an unpolarized nucleon target is given by [39]

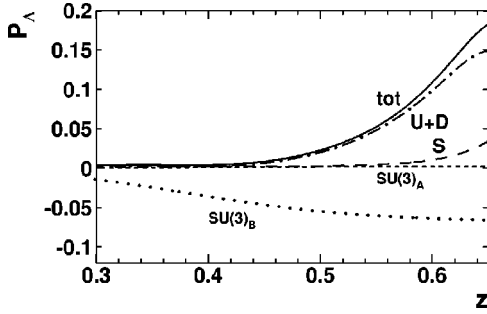


FIG. 9. The polarization of the  $\Lambda$  produced in semi-inclusive, polarized  $e^-p$  scattering. The results were calculated for  $E_e=30$  GeV,  $x=0.3$ , and  $Q^2=10$  GeV $^2$ . The electron polarization is arbitrarily set to 50%. The contributions from the fragmentation of  $u+d$  and  $s$  quarks are shown as dash-dotted and dashed lines, respectively. The solid line is the total polarization. The predictions of the flavor symmetric models (A) and (B) are shown as short dashed and dotted lines, respectively.

$$\tilde{P}_\Lambda = \hat{e}_3 P_e \frac{y(2-y)}{1+(1-y)^2} \frac{\sum_q e_q^2 q_N(x, Q^2) \Delta D_{q\Lambda}(z, Q^2)}{\sum_q e_q^2 q_N(x, Q^2) D_{q\Lambda}(z, Q^2)}, \quad (30)$$

where  $y \equiv (E-E')/E$  is the usual DIS variable and  $z \equiv p_\Lambda \cdot p_N / p_N \cdot p$  where  $p_\Lambda$ ,  $p_N$  and  $q$  are the four-momenta of the  $\Lambda$ , nucleon and the virtual photon. The electron beam defines the  $\hat{e}_3$  axis and  $P_e$  is the degree of polarization of the incident electron. At not too small Bjorken  $x$  values the contributions from strange quarks may be neglected, and  $P_\Lambda$  measures effectively  $\Delta D_{u\Lambda}/D_{u\Lambda}$ . We calculated the  $\Lambda$  polarization using our fragmentation functions. Figure 9 shows the result calculated at  $E_e \approx 30$  GeV,  $x=0.3$  and  $Q^2=10$  GeV $^2$ , where  $y=0.58$ . A beam polarization of 50% was assumed. The dash-dotted and dashed lines are contributions from the fragmentation of  $u$  plus  $d$  quarks and  $s$  quarks, respectively. The solid line is the total polarization. We see that the polarization is positive and large for higher  $z$  values, and that the dominant contributions come from the fragmentation of up quarks. At even larger  $z$  values, the contribution of strange quarks becomes important since  $\Delta D_{s\Lambda}$  is harder than  $\Delta D_{u\Lambda}$ , as can be seen from Fig. 2. However, since the cross section decreases rapidly with increasing  $z$ , the bulk of the produced  $\Lambda$ 's are fragmentation products of  $u$  quarks. Thus, in semi-inclusive scattering of polarized electrons from nucleons, a positive value of  $P_\Lambda$  at intermediate values of  $z$  would confirm our prediction. Although the absolute values of  $\Delta D_{u\Lambda}$  are quite small, they lead to a relatively large polarization since, in the limit  $z \rightarrow 1$ , the component of the wave function containing a scalar diquark dominates both  $\Delta D_{u\Lambda}$  and  $D_{u\Lambda}$ . In Fig. 9, we also show the predictions resulting from flavor symmetric fragmentation functions for both cases (A) and (B). While (A) gives essentially zero  $\Lambda$  polarization, (B) predicts a negative  $\Lambda$  polarization due to the fragmentation of negatively polarized up quarks. Thus, polarization measurements in semi-inclusive DIS can

easily differentiate between our predictions and those obtained from flavor symmetric models.

## V. CONCLUSIONS

We discussed the quark parton structure of the  $\Lambda$  baryon and the fragmentation of quarks into a  $\Lambda$ . Starting from the general definition of quark distributions and fragmentation functions, which explicitly incorporates energy momentum conservation, we were able to show the following:

(i) The hyperfine interaction responsible for the  $\Delta$ - $N$  and  $\Sigma$ - $\Lambda$  mass splitting leads to quark distributions and fragmentation functions which differ significantly from those based on  $SU(3)$  and  $SU(6)$  symmetries.

(ii) The hyperfine interaction leads to two main qualitative predictions for lambda quark distributions and quark fragmentation functions.

First, it implies that the strange quark distribution in the  $\Lambda$  and the strange quark fragmentation functions into a Lambda are much harder than the corresponding up and down quark distributions and fragmentation functions.

Second, it predicts that the non-strange valence quarks of the  $\Lambda$  are polarized and hence that non-strange quarks can fragment into polarized lambda's.

(iii) The relative magnitude of the non-strange quark polarization is substantial for large Bjorken  $x$  values, where both the polarized and the unpolarized quark distributions are governed by the scalar diquark component of the wave function. This large non-strange polarization will dominate any observable in which the strange component is suppressed.

Our approach also gives a natural explanation for the dependence of the maximum of the  $\xi = \ln(1/z)$  spectrum on the type of particles produced in  $e^+e^-$  annihilation.

While all these associations follow quite naturally from the general definitions of the quark distributions and fragmentation functions and energy-momentum conservation, the magnitude of these effects has to be calculated in a model-dependent way. We calculated the quark distribution and fragmentation functions in the MIT bag model, using the Peierls-Yoccoz projection method to construct translationally invariant states. The calculated fragmentation functions give an overall good description of all measured observables and are in far better agreement with the data than flavor symmetric models. We predict positive and significant  $\Lambda$  polarization in semi-inclusive DIS experiments induced by charged leptons, while models based on  $SU(3)$  flavor symmetry predict zero or negative  $\Lambda$  polarization.

## ACKNOWLEDGMENTS

We would like to thank W. Melnitchouk, A.W. Schreiber and K. Tsushima for helpful discussions. This work was partly supported by the Australian Research Council. One of the authors (J.T.L.) was supported in part by National Science Foundation research contract PHY-9722706. One author (J.T.L.) wishes to thank the Special Research Center for the Subatomic Structure of Matter for its hospitality during the time this work was carried out.

- [1] E. D. Bloom *et al.*, Phys. Rev. Lett. **23**, 930 (1969).  
[2] EMC Collaboration, J. Ashman *et al.*, Phys. Lett. B **206**, 364 (1988).  
[3] E143 Collaboration, K. Abe *et al.*, Phys. Rev. Lett. **74**, 346 (1995).  
[4] SMC Collaboration, D. Adams *et al.*, Phys. Lett. B **329**, 399 (1994).  
[5] Hermes Collaboration, A. Airapetian *et al.*, Phys. Lett. B **442**, 484 (1998).  
[6] J. Ellis and R. L. Jaffe, Phys. Rev. D **9**, 1444 (1974).  
[7] M. Burkardt and R.L. Jaffe, Phys. Rev. Lett. **70**, 2537 (1993).  
[8] I. Bigi, Nuovo Cimento A **41**, 43 (1977).  
[9] J. F. Donoghue, Phys. Rev. D **17**, 2922 (1978).  
[10] A. Bartl, H. Fraas, and R. Majoretto, Z. Phys. C **6**, 335 (1980); **9**, 181 (1981).  
[11] G. Gustavson and J. Häkkinen, Phys. Lett. B **303**, 350 (1993).  
[12] W. Melnitchouk and A. W. Thomas, Z. Phys. A **353**, 311 (1995).  
[13] W. Lu and B.-Q. Ma, Phys. Lett. B **357**, 419 (1995); W. Lu, *ibid.* **373**, 223 (1996).  
[14] J. Ellis, D. Kharzeev, and A. Kotzinian, Z. Phys. C **69**, 467 (1996); M. Alberg, J. Ellis, and D. Kharzeev, Phys. Lett. B **356**, 113 (1995).  
[15] W. Lu, X. Li, and H. Hu, Phys. Rev. D **53**, 131 (1996).  
[16] Z. Liang and C. Boros, Phys. Rev. Lett. **79**, 3608 (1997).  
[17] D. de Florian, M. Stratmann, and W. Vogelsang, Phys. Rev. Lett. **81**, 530 (1998).  
[18] D. de Florian, M. Stratmann, and W. Vogelsang, Phys. Rev. D **57**, 5811 (1998).  
[19] C. Boros and Z. Liang, Phys. Rev. D **57**, 4491 (1998).  
[20] D. de Florian *et al.*, Phys. Lett. B **439**, 176 (1998).  
[21] A. Kotzinian, A. Bravar, and D. von Harrach, Eur. Phys. J. C **2**, 329 (1998).  
[22] B. Ma and J. Soffer, Phys. Rev. Lett. **82**, 2250 (1999).  
[23] M. Alberg *et al.*, Phys. Lett. B **389**, 367 (1996).  
[24] C. Boros and A. W. Thomas, Phys. Rev. D **60**, 074017 (1999).  
[25] F. E. Close, Phys. Lett. **43B**, 422 (1973).  
[26] R. Carlitz and J. Kaur, Phys. Rev. Lett. **38**, 673 (1977).  
[27] F. E. Close and A. W. Thomas, Phys. Lett. B **212**, 227 (1988).  
[28] G. R. Farrar and D. R. Jackson, Phys. Rev. Lett. **35**, 1416 (1975).  
[29] S. J. Brodsky, M. Burkardt, and I. Schmidt, Nucl. Phys. **B441**, 197 (1995).  
[30] W. Melnitchouk and A. W. Thomas, Phys. Lett. B **377**, 11 (1996).  
[31] U. K. Yang and A. Bodek, Phys. Rev. Lett. **82**, 2467 (1999).  
[32] M. Nzar and P. Hoodbhoy, Phys. Rev. D **51**, 32 (1995).  
[33] R. Jakob, P. J. Mulders, and J. Rodrigues, Nucl. Phys. **A626**, 937 (1997).  
[34] B. Ma, I. Schmidt, and J. Yang, hep-ph/9906424; Phys. Rev. D. (to be published), hep-ph/9907224.  
[35] J. C. Collins and D. E. Soper, Nucl. Phys. **B194**, 445 (1982).  
[36] R. L. Jaffe, Nucl. Phys. **B229**, 205 (1983).  
[37] A. I. Signal and A. W. Thomas, Phys. Lett. B **211**, 481 (1988); Phys. Rev. D **40**, 2832 (1989); A. W. Schreiber *et al.*, *ibid.* **42**, 2226 (1990).  
[38] A. W. Schreiber, A. I. Signal, and A. W. Thomas, Phys. Rev. D **44**, 2653 (1991).  
[39] R. L. Jaffe, Phys. Rev. D **54**, 6581 (1996).  
[40] R. L. Jaffe and X. Ji, Phys. Rev. Lett. **71**, 2547 (1993).  
[41] DELPHI Collaboration, W. Adam *et al.*, Z. Phys. C **69**, 561 (1996).  
[42] L3 Collaboration, M. Acciarri *et al.*, Phys. Lett. B **328**, 223 (1994); **371**, 126 (1996); **393**, 465 (1997).  
[43] Opal Collaboration, K. Ackerstaff *et al.*, Eur. Phys. J. C **8**, 241 (1999).  
[44] SLD Collaboration, K. Abe *et al.*, Phys. Rev. D **59**, 052001 (1999).  
[45] Yu. L. Dokshitzer, V. A. Khoze, A. H. Mueller, and S. I. Troyan, *Basics of Perturbative QCD* (Editions Frontières, Gif-sur-Yvette, 1991), and references therein.  
[46] ALEPH Collaboration, D. Buskulic *et al.*, Z. Phys. C **64**, 361 (1994).  
[47] DELPHI Collaboration, P. Abreu *et al.*, Phys. Lett. B **318**, 249 (1993).  
[48] L3 Collaboration, M. Acciarri *et al.*, Phys. Lett. B **407**, 389 (1997).  
[49] Opal Collaboration, G. Alexander *et al.*, Z. Phys. C **73**, 569 (1997).  
[50] J. F. Owens, Phys. Lett. **76B**, 85 (1978); T. Uematsu, *ibid.* **79B**, 97 (1978).  
[51] G. Altarelli *et al.*, Nucl. Phys. **B160**, 301 (1970); P. Nason and B. Webber, *ibid.* **B421**, 473 (1994); **B480**, 755(E) (1996).  
[52] M. Miyama and S. Kumano, Comput. Phys. Commun. **94**, 185 (1996); M. Hirai, S. Kumano, and M. Miyama, *ibid.* **108**, 38 (1998).  
[53] ALEPH Collaboration, D. Buskulic *et al.*, Phys. Lett. B **374**, 319 (1996).  
[54] DELPHI Collaboration, K. Ackerstaff *et al.*, Eur. Phys. J. C **2**, 49 (1998).  
[55] T. Sjöstrand, Comput. Phys. Commun. **82**, 74 (1994).  
[56] B. Anderson *et al.*, Phys. Rep. **97**, 45 (1982).